JOURNAL OF VIROLOGY, July 2011, p. 6702–6713 Vol. 85, No. 13
0022-538X/11/$12.00 doi:10.1128/JVI.00200-11

Shifting Hierarchies of Interleukin-10-Producing T Cell Populations in the Central Nervous System during Acute and Persistent Viral Encephalomyelitis[▽]

Shweta S. Puntambekar,[1] Cornelia C. Bergmann,[1] Carine Savarin,[1] Christopher L. Karp,[2] Timothy W. Phares,[1] Gabriel I. Parra,[1] David R. Hinton,[3] and Stephen A. Stohlman[1]*

Department of Neurosciences, Lerner Research Institute, The Cleveland Clinic Foundation, Cleveland,[1] and Division of Molecular Immunology, Cincinnati Children's Hospital Research Foundation, Cincinnati,[2] Ohio, and Department of Pathology, The University of Southern California Keck School of Medicine, Los Angeles, California[3]

Received 28 January 2011/Accepted 18 April 2011

Interleukin-10 (IL-10) mRNA is rapidly upregulated in the central nervous system (CNS) following infection with neurotropic coronavirus and remains elevated during persistent infection. Infection of transgenic IL-10/green fluorescent protein (GFP) reporter mice revealed that CNS-infiltrating T cells were the major source of IL-10, with minimal IL-10 production by macrophages and resident microglia. The proportions of IL-10-producing cells were initially similar in $CD8^+$ and $CD4^+$ T cells but diminished rapidly in $CD8^+$ T cells as the virus was controlled. Overall, the majority of IL-10-producing $CD8^+$ T cells were specific for the immunodominant major histocompatibility complex (MHC) class I epitope. Unlike $CD8^+$ T cells, a large proportion of $CD4^+$ T cells within the CNS retained IL-10 production throughout persistence. Furthermore, elevated frequencies of IL-10-producing $CD4^+$ T cells in the spinal cord supported preferential maintenance of IL-10 production at the site of viral persistence and tissue damage. IL-10 was produced primarily by the $CD25^+$ $CD4^+$ T cell subset during acute infection but prevailed in $CD25^-$ $CD4^+$ T cells during the transition to persistent infection and thereafter. Overall, these data demonstrate significant fluidity in the T-cell-mediated IL-10 response during viral encephalitis and persistence. While IL-10 production by $CD8^+$ T cells was limited primarily to the time of acute effector function, $CD4^+$ T cells continued to produce IL-10 throughout infection. Moreover, a shift from predominant IL-10 production by $CD25^+$ $CD4^+$ T cells to $CD25^-$ $CD4^+$ T cells suggests that a transition to nonclassical regulatory T cells precedes and is retained during CNS viral persistence.

A variety of viruses evade complete immune-mediated clearance, resulting in persistent infection (14, 16). Specifically beneficial for viral persistence are host mechanisms designed to regulate excessive immune responses and limit tissue damage. One of the nonredundant mediators regulating immune-mediated damage and facilitating repair is the anti-inflammatory cytokine interleukin-10 (IL-10) (13, 15, 29, 30). Production of IL-10 following immune cell recruitment into sites of inflammation limits macrophage and dendritic cell activation and maturation, resulting in suppression of sustained T cell function (13, 15, 29). IL-10 can be secreted by a wide range of cells, including macrophages, dendritic cells, B cells, and various subsets of $CD8^+$ and $CD4^+$ T cells (2, 13, 29). The role of IL-10 differs dramatically in distinct viral infections, potentially reflecting different magnitudes, sources, and temporal responses. For example, IL-10 expressed primarily by effector $CD8^+$ and $CD4^+$ T cells does not affect the clearance of influenza virus from the lungs (33, 39). However, IL-10 is vital in preventing excessive monocytic inflammation and potentially lethal pulmonary injury (39). In contrast, IL-10 limits the clearance of murine gammaherpesvirus 68 (32), lymphocytic choriomeningitis virus (LCMV) (10, 14), and vaccinia virus (43). IL-10 production within T cells is transiently upregulated following LCMV infection and is subsequently downregulated concomitantly with the loss of T cell function (8, 10, 14). However, during persistent LCMV infection, IL-10 production by dendritic cells is associated with altered T cell function, facilitating viral persistence (10, 15, 17). The presence of IL-10 during acute inflammation may thus limit immune-mediated damage without affecting viral control, while sustained IL-10 expression may counteract antiviral T cell effector function during persistence. The mechanisms underlying IL-10 production by distinct cell types and their influence on virus clearance and virus-induced pathology still remain to be defined for many viral diseases.

Infection with the neurotropic JHM strain of mouse hepatitis virus (JHMV) induces an acute encephalomyelitis that resolves into a persistent infection confined to the central nervous system (CNS) (5). JHMV infects various CNS cell types, resulting in the recruitment of both innate and adaptive immune components (5). $CD8^+$ T cells are the primary effectors of virus clearance, using perforin and gamma interferon (IFN-γ) to control viral replication in distinct CNS cell populations (5). While the virus is eliminated from astrocytes and microglia via a perforin-dependent mechanism, IFN-γ controls the infection of oligodendroglia (5, 6). During acute encephalomyelitis, IL-10 is upregulated as an early response to JHMV infection (31), as in a variety of human and rodent viral infections (8, 15). Recent data suggest that IL-10 secretion by $CD8^+$ T cells correlates with antiviral activity (41).

* Corresponding author. Mailing address: Department of Neuroscience, Lerner Research Institute, The Cleveland Clinic, 9500 Euclid Avenue, NC30, Cleveland, OH 44195. Phone: (216) 445-9796. Fax: (216) 444-7927. E-mail: stohlms2@ccf.org.

▽ Published ahead of print on 27 April 2011.

However, the role of IL-10 in regulating the clearance of infectious virus from the CNS is unclear. In contrast to the neutral or opposing antiviral effects of IL-10 in non-CNS infections, inhibition of IL-10 facilitates viral control in the CNS during acute infection (26). By contrast, analysis of JHMV infection in IL-10-deficient mice suggests that IL-10 limits viral clearance (41). Recruitment of regulatory T cells (Treg) secreting IL-10 within the infected CNS represents a potential host defense mechanism to control exaggerated immune responses and thereby limit immune pathology. Indeed, depletion of Treg during acute JHMV infection increases mortality (1), while adoptive transfer of Treg partially rescues this effect, diminishing clinical severity and demyelination (1, 40, 41). Interestingly, adoptive transfer of $CD4^+$- and/or $CD8^+$-enriched T cell populations into JHMV-infected IL-10-deficient mice decreases demyelination (41), suggesting that multiple cellular sources of IL-10 may play synergistic roles in the regulation of viral persistence within the CNS. Persistence is characterized by the presence of viral antigen and RNA in the absence of detectable infectious virus, predominantly in the spinal cord (5, 25). In contrast to acute systemic infections that resolve into viral persistence correlated with T cell exhaustion (8, 9, 22), JHMV-specific $CD8^+$ T cells maintain the ability to secrete IFN-γ during persistence (3, 5).

To understand a potential association between persisting JHMV infection and IL-10, this report characterizes the kinetics of IL-10 production and the cell types producing IL-10 within the CNS during JHMV pathogenesis by using a transgenic IL-10 reporter mouse. In contrast to systemic infections (8, 10, 14, 33), little or no IL-10 production was detected in cells of the myeloid lineage; however, both CNS-infiltrating $CD4^+$ and $CD8^+$ T cells produced IL-10. The proportions of IL-10-producing cells were initially similar in the $CD8^+$ and $CD4^+$ T cell compartments in the CNS. Virus-specific $CD8^+$ T cells contained a higher frequency of IL-10-producing cells than did $CD8^+$ T cells of unknown specificity. Nevertheless IL-10 production diminished rapidly in $CD8^+$ T cells as the virus was controlled. By contrast, IL-10 production was sustained by a large proportion of $CD4^+$ T cells, with IL-10-producing $CD4^+$ T cells most prominent in the spinal cord, the primary site of viral persistence. Finally, while $CD25^+$ $CD4^+$ T cells constituted the major IL-10-producing subpopulation during acute infection, IL-10 production prevailed in the $CD25^-$ $CD4^+$ T cell subset during the transition to persistent infection and thereafter. The data demonstrate that distinct T cell populations dominate as sources of IL-10 during the course of CNS viral infection. IL-10-mediated dampening of immune responses may thus mitigate immunopathology, thereby preventing mortality but contributing to viral persistence within the CNS.

MATERIALS AND METHODS

Mice and virus infection. Wild-type (wt) C57BL/6 mice were purchased from the National Cancer Institute (Frederick, MD). IL-10/GFP (green fluorescent protein) reporter mice, designated Vert-X mice, on the C57BL/6 background (27, 39) were bred locally under pathogen-free conditions. Mice were infected at the age of 6 to 7 weeks by intracranial injection of 250 PFU of the monoclonal antibody (MAb) escape mutant of JHMV designated V2.2 (19). Animals were scored daily for clinical signs based on the scoring system previously described (19): 0, healthy; 1, ruffled fur and hunched back; 2, hind-limb paralysis/inability to turn to an upright position; 3, complete hind-limb paralysis and wasting; 4, moribund/dead. All procedures were conducted under protocols approved by the Institutional Animal Care and Use Committee.

Isolation of mononuclear cells. Mononuclear cells were isolated from the CNS as described previously (3, 6, 34). Briefly, tissues were homogenized in phosphate-buffered saline (PBS) using ice-cold Ten Broeck tissue grinders. Homogenates were centrifuged at 450 × *g* for 7 min at 4°C. Supernatants were stored at −80°C for determination of virus titers. Cells were resuspended in cold RPMI 1640 supplemented with 25 mM HEPES (pH 7.2), adjusted to 30% Percoll (Pharmacia, Piscataway, NJ), and centrifuged at 800 × *g* for 30 min at 4°C onto a 70% Percoll cushion. Cells were recovered from the 30%–70% interface, washed with RPMI containing 25 mM HEPES, and resuspended in fluorescence-activated cell sorting (FACS) buffer (PBS with 0.5% bovine serum albumin [BSA]). Viable cell numbers were determined by trypan blue exclusion, and a minimum of 5×10^5 cells were used for flow cytometric analysis. Single-cell suspensions from cervical lymph nodes (CLN) were prepared as described previously (3, 34). CNS monocyte-derived $CD45^{hi}$ $CD11b^+$ macrophages, $CD45^{lo}$ microglia, and $CD3^+$ T cells were purified from pooled brains using a BD FACSAria flow cytometer (BD Biosciences, San Diego, CA). In brief, brains ($n = 6$) were finely minced and digested with 0.25% trypsin in PBS for 30 min at 37°C (34). Trypsin activity was terminated by the addition of 20% newborn calf serum and the mononuclear cells enriched by Percoll gradient centrifugation as described above. A minimum of 10^5 cells were collected per sample and were frozen in 400 μl of Trizol (Invitrogen, Carlsbad, CA) at −80°C for subsequent RNA extraction and PCR analysis (see below).

Cell staining and flow cytometric analysis. Cells were incubated with mouse serum and a rat anti-mouse FcγIII/II MAb (2.4G2; BD Biosciences, San Diego, CA) for 20 min on ice prior to staining to eliminate nonspecific binding. GFP expression was analyzed in the fluorescein isothiocyanate (FITC)/FL1 channel. Cell type-specific expression of surface antigens was determined by incubation with either a phycoerythrin (PE)-, an FITC-, a peridinin chlorophyll protein (PerCP)-, or an allophycocyanin-conjugated MAb specific for CD45 (30-F11), CD11b (M1/20), CD3 (145.2c11), CD4 (L3T4), CD8 (53-6.7), CD25 (PC61) (all from BD PharMingen), or F4/80 (Serotec, Raleigh, NC) for 30 min on ice. Virus-specific $CD8^+$ T cells were identified using D^b/S510 major histocompatibility complex class I tetramers (3, 4) (Beckman Coulter, Fullerton, CA). Intracellular Foxp3 was detected by staining for cell surface markers, permeabilization with Fixation/Permeabilization reagent (eBioscience, San Diego CA), and incubation with PE-labeled anti-Foxp3 (FJK-16S; eBioscience) as recommended by the supplier. Cells derived from Vert-X IL-10/GFP reporter mice were analyzed without fixation on a FACSCalibur flow cytometer (BD Biosciences). Data were analyzed using FlowJo software (version 7.6.1; Tree Star Inc., Ashland, OR).

Virus titer determination. Virus titers were determined in clarified supernatants of homogenized brains by plaque assays using the murine delayed brain tumor (DBT) astrocytoma as detailed previously (3, 6, 26). Plaques were counted after 48 h of incubation at 37°C.

Histopathology. Tissues were fixed in 10% formalin and were embedded in paraffin. The distribution of viral antigen was determined by immunoperoxidase staining using the anti-nucleocapsid MAb J.3.3 (6, 25, 36) as the primary antibody (Ab), a horse anti-mouse Ab as the secondary Ab, and 3,3′-diaminobenzidine as a substrate (Vectastain-ABC kit; Vector Laboratories, Burlingame, CA). Inflammation was determined by staining with hematoxylin and eosin (H&E). Demyelination was determined by staining with luxol fast blue (LFB). Sections were scored in a blinded fashion, and representative fields were identified based on the average score of all sections in each experimental group. Stained tissue sections on glass slides were scanned with an Aperio (Vista, CA) ScanScope at a magnification of ×40 and were digitally imaged at high resolution.

Real-time PCR analysis. Snap-frozen brains and spinal cords from individual mice ($n = 3$ to 4) were homogenized using Ten Broeck glass grinders in Trizol (Invitrogen), and the RNA was isolated as described previously (24, 34). DNA contamination was removed by treatment with DNase I for 30 min at 37°C (DNA-free kit; Ambion, Austin, TX), and cDNA was synthesized from RNA using Moloney murine leukemia virus (M-MLV) reverse transcriptase (Invitrogen) and oligo(dT) primers (Promega, Madison, WI). Quantitative real-time PCR (qRT-PCR) was performed using 4 μl of cDNA and SYBR green master mix (Applied Biosystems, Foster City, CA) in duplicate on a 7500 Fast real-time PCR system (Applied Biosystems). PCR conditions were 10 min at 95°C followed by 40 cycles of 95°C for 15 s, 60°C for 30 s, and 72°C for 30s. Real-time primer sequences were as follows: GAPDH (glyceraldehyde-3-phosphate dehydrogenase) sense, 5′-CATGGCCTTCCGTGTTCCTA-3′; GAPDH antisense, 5′-ATGCCTGCTTCACCACCTTCT-3′; IL-10 sense, 5′-TTTGAATTCCCTGGGTGAGAA-3′; IL-10 antisense, 5′-GCTCCACTGCCTTGCTCTTATT-3′; JHMV nucleocapsid (N) gene sense, 5′-CGCAGAGTATGGCGACGAT-3′; JHMV N gene antisense, 5′-GAGGTCCTAGTCTCGGCCTGTT-3′. IFN-γ mRNA levels

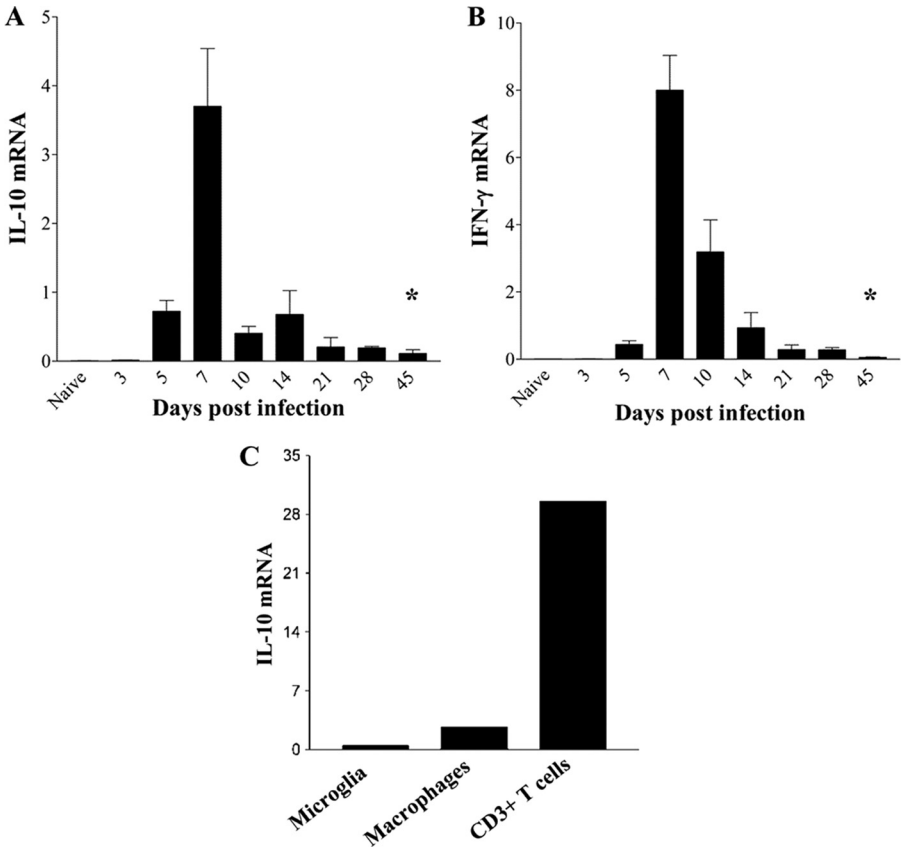

FIG. 1. IL-10 mRNA expression during viral encephalomyelitis. (A and B) RNA extracted from brains of JHMV-infected mice at various times p.i. was assessed for expression of IL-10 (A) and IFN-γ (B) mRNA by qRT-PCR. Expression in naïve brains is 0.006 ± 0.0006 for IL-10 mRNA and 0.009 ± 0.001 for IFN-γ mRNA. Data are means ± SEM for 3 individual mice and are expressed relative to the level of GAPDH mRNA. Asterisks indicate significant differences (*, $P < 0.05$) from results for naïve mice. (C) IL-10 mRNA expression in purified microglia, macrophages, and $CD3^+$ T cells derived from JHMV-infected brains at day 10 p.i. Expression levels relative to those of GAPDH are representative of 2 experiments with 3 to 5 pooled mice.

were determined relative to the level of GAPDH mRNA by using Applied Biosystems gene expression arrays with Universal TaqMan Fast master mix (Applied Biosystems). PCR conditions were 20 s at 95°C followed by 40 cycles of 95°C for 3 s and 60°C for 30 s. Transcript levels were calculated relative to the levels of the housekeeping gene GAPDH using the formula $2[C_T(\text{GAPDH}) - C_T(\text{target gene})] \times 1{,}000$, where C_T is determined as the threshold cycle at which the fluorescent signal becomes significantly higher than that of the background.

Statistical analysis. Results are expressed as means ± standard errors of the means (SEM) for each group of mice. Statistics were determined using a standard two-tailed Student *t* test. Graphs were plotted using GraphPad Prism software (version 3.0) and Microsoft Excel.

RESULTS

Pathogenesis in IL-10 reporter mice. IL-10 mRNA and protein peak in the CNS during acute infection with both lethal and sublethal variants of JHMV (24, 31) concomitantly with maximal cellular inflammation (3, 5, 21, 24, 31). To determine whether IL-10 expression was sustained during viral persistence, wt mice were infected with a sublethal variant of JHMV, and IL-10 mRNA expression was examined in brains throughout acute and persistent infection. IL-10 mRNA levels increased rapidly by day 5 postinfection (p.i.), reached maximal expression at day 7 p.i., and declined rapidly thereafter (Fig. 1A). Although infectious virus was no longer detected after day 14 p.i. in wt mice (3, 5, 19) (data not shown), IL-10 mRNA remained stably elevated at levels 10- to 20-fold higher than those for uninfected mice throughout day 45 p.i. (Fig. 1A). Ongoing, sustained IL-10 mRNA levels, despite viral control, implicated IL-10 production as a consequence of immunopathology, possibly in conjunction with persisting T cell stimulation by viral antigen. Indeed, kinetic analysis of IFN-γ mRNA, dependent on a direct T-cell receptor (TcR)–target cell interaction (38), revealed a similar abrupt decline in the level of IFN-γ mRNA after day 7 p.i., but IFN-γ mRNA also remained elevated throughout persistence (Fig. 1B). While IFN-γ is produced mainly by T cells in the CNS during JHMV infection (5, 20), a variety of both inflammatory and resident cells are capable of IL-10 production (2, 8, 12, 22, 29). To determine the primary source of IL-10 during acute infection, IL-10 mRNA expression was compared in $CD45^{lo}$ microglia, $CD45^{hi}$ $CD11b^+$ monocytes/macrophages, and $CD45^{hi}$ $CD3^+$ T cells purified from the CNSs of JHMV-infected mice. Neither resident microglia nor the infiltrating macrophage population expressed significant amounts of IL-10 mRNA relative to those in $CD3^+$ T cells (Fig. 1C). These results implicated T cells as the major contributors to IL-10 production during acute JHMV infection.

To define more clearly the cell types producing IL-10 during

virally induced encephalomyelitis, JHMV pathogenesis was characterized in IL-10 reporter mice that coexpress IL-10 and GFP (27). The disease incidence, day of onset, and progression of clinical symptoms, which include early signs of encephalitis followed by hind-limb paralysis gradually resolving with time, were typical of JHMV infection of syngeneic wt mice (5) (data not shown). The level of infectious virus in the CNS was maximal at day 7 p.i. and was subsequently controlled by day 14 p.i. (Fig. 2A), with kinetics similar to those for wt mice (5). Following the clearance of infectious virus, JHMV persisted in the CNSs of infected IL-10 reporter mice (Fig. 2B) at levels similar to those in wt mice (3, 4, 5). The foci of viral antigen and inflammation at day 7 p.i. were typical of acute JHMV-induced encephalitis (Fig. 2C and D). At day 14 p.i., viral antigen was prominent within the white matter of the spinal cord in cells with the morphological appearance of oligodendroglia (Fig. 2E). There was no evidence for infection of cells with the appearance of astrocytes or neurons. In addition, both cellular infiltration and demyelination, a hallmark of JHMV infection (5), were evident in white-matter tracks (Fig. 2F). JHMV infection persisted in the white-matter tracks of the IL-10 reporter mice following the clearance of infectious virus at days 21 and 30 p.i., with scattered infected cells in and around the focal areas of demyelination (Fig. 2G and H), a feature characteristic of persistent JHMV infection (5). These data indicate that IL-10 reporter transgene expression did not alter the antiviral response or viral pathogenesis exhibited by wt mice.

Inflammatory lymphocytes are the major IL-10-producing population during JHMV infection. JHMV infection elicits a robust CNS inflammatory response characterized by glial cell activation and infiltration by monocytes, neutrophils, NK cells, T cells, and B cells (5). Unaltered JHMV pathogenesis in IL-10 reporter mice facilitated the direct identification of cell subsets that secrete IL-10 without *in vitro* restimulation. While monocytes and neutrophils are recruited from bone marrow (5), T cells are activated in the CLN prior to trafficking into the CNS (28). However, the frequency of activated IL-10-producing T cells in CLN was extremely low throughout acute infection (<0.05% [data not shown]). The uninfected CNS has very low basal levels of $CD45^{hi}$ cells (<1% [data not shown]). By contrast, IL-10-producing cells within the CNS were readily detected throughout infection, and the vast majority were characterized by high CD45 expression (Fig. 3A). In the inflamed CNS, high CD45 expression marks all infiltrating cells of bone marrow origin, with the highest expression on T and NK cells relative to slightly reduced expression on monocytes, neutrophils, and B cells (3, 20, 21, 24, 34, 40). CNS-resident microglia, in contrast, have a $CD45^{lo}$ phenotype (36). Cells expressing high IL-10 levels were thus most likely T lymphocytes (Fig. 3A), consistent with the RNA analysis of cells purified from the inflamed CNS (Fig. 1C). CNS infiltration by $CD45^{hi}$ inflammatory cells peaked at 7 days p.i. and declined as infectious virus was controlled (Fig. 3A and B). The relative proportion of IL-10-producing cells peaked with a slight delay at ~15% to 20% of $CD45^{hi}$ inflammatory cells (Fig. 3A) and 5 to 8% of total cells between days 10 and 14 p.i. (Fig. 3C). Although the frequencies of total-cell yields (Fig. 3B), inflammatory cells (Fig. 3C), and inflammatory IL-10-producing cells (Fig. 3C) declined during the transition from acute to persistent infection, IL-10-producing cells were retained within the $CD45^{hi}$ population to at least day 31 p.i. during viral persistence (Fig. 3A and C). Consistent with the analysis of IL-10 mRNA expression (Fig. 1C), few if any $CD45^{lo}$ microglia expressed IL-10 at any time p.i. Similarly, examination of $CD11b^+$ $F4/80^+$ macrophages recruited into the CNS showed only a low intensity of IL-10 expression in a small proportion of cells, which increased from ~7% to 16% of macrophages between days 7 and 14 p.i. but subsided by day 31 p.i. (Fig. 4A and C). Overall, the frequency of IL-10-producing macrophages remained below 4% of the total infiltrating cells (Fig. 4B). These results, coupled with the minimal expression of IL-10 mRNA in microglia and macrophages, suggest that signals inducing IL-10 production by myeloid cells are minimal in the inflamed CNS. The rapid decline in the percentage of $CD45^{hi}$ monocytes (Fig. 4B), coincident with that of IL-10-producing lymphocytes Fig. 3A and C, is reminiscent of pulmonary viral infection, in which IL-10 is associated with ameliorated myeloid cell recruitment (39). The data thus support IL-10 production during acute inflammation as a host response to limit ongoing inflammation (13, 29).

Distinct regulation of IL-10 production by $CD8^+$ and $CD4^+$ T cells. To confirm T cells as primary sources of IL-10 during JHMV-induced encephalomyelitis, IL-10 production was monitored in both $CD8^+$ and $CD4^+$ T cells infiltrating the CNS. $CD8^+$ T cells are the primary immune effectors controlling infectious JHMV within the CNS (3, 5, 6), while $CD4^+$ T cells enhance the survival and effector function of $CD8^+$ T cells (3, 5, 6). Both subsets are critical for optimal viral clearance but are also mediators of pathology (6, 35, 42). Although the percentage of $CD45^{hi}$ cells declined during the transition from acute to persistent infection (Fig. 3), the overall proportion of $CD8^+$ T cells within the $CD45^{hi}$ inflammatory population in brains remained stable at ~25 to 30% throughout infection (Fig. 5A and B). Importantly, ~20% of $CD8^+$ T cells produced IL-10 during acute infection; however, the relative frequency of $CD8^+$ T cells producing IL-10 during persistence declined 2-fold, to ~10%, by day 31 p.i.

$CD4^+$ T cell levels were initially lower than those of $CD8^+$ T cells but increased as infectious virus was controlled, constituting ~50% of the infiltrates at day 14 p.i. (Fig. 5A and C). The relative frequencies of IL-10-producing cells within the $CD4^+$ T cell population were similar to those in $CD8^+$ T cells to day 10 p.i. However, in contrast to the decline in the proportion of $IL\text{-}10^+$ $CD8^+$ T cells, the proportion of $IL\text{-}10^+$ cells within $CD4^+$ T cells increased to a stable level of ~30% during viral persistence (Fig. 5A). Moreover, analysis of mean fluorescence intensity (MFI) as a readout for relative IL-10 production indicated significantly higher IL-10 expression by $CD4^+$ T cells than by $CD8^+$ T cells at the population level (Fig. 5A). Comparison of the relative frequencies of IL-10-producing $CD8^+$ versus $CD4^+$ T cells within the $CD45^{hi}$ CNS infiltrates clearly demonstrates the distinct kinetics throughout infection (Fig. 5B and C). $IL\text{-}10^+$ $CD8^+$ T cells prevail early and start declining at day 14 p.i. Like $IL\text{-}10^+$ $CD8^+$ T cells, $IL\text{-}10^+$ $CD4^+$ T cells constitute ~5% of the inflammatory response at day 7 p.i. However, this population increases to ~15% of the total infiltrate between days 10 and 21 p.i., comprising the predominant IL-10 anti-inflammatory activity within the CNS as the virus is controlled and during chronic infection.

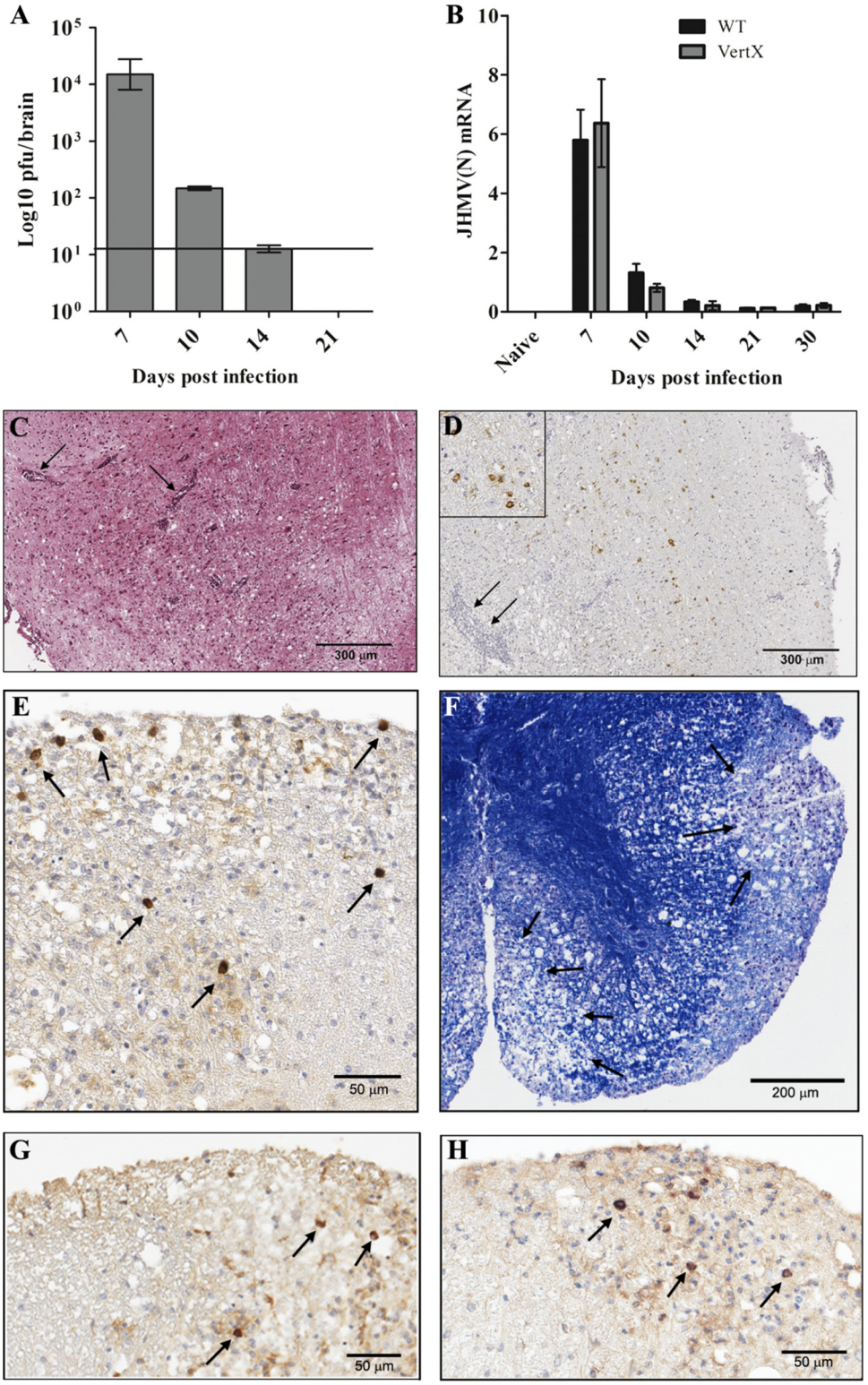

FIG. 2. JHMV pathogenesis in transgenic IL-10 reporter mice. (A) Levels of infectious virus in the CNS of IL-10 reporter mice determined by plaque assays of brain homogenates from 3 to 4 individual mice at various times p.i. The horizontal line represents the limit of detection. (B) JHMV nucleocapsid (N) mRNA expression in brains of infected IL-10 reporter (shaded bars) and wt (filled bars) mice at various times p.i. Data are expressed relative to the level of GAPDH mRNA. (C) Foci of inflammatory infiltrates (arrows) within the brain at day 7 p.i. H&E staining was used. (D) Viral antigen foci in the brain at day 7 p.i. Arrows show inflammatory infiltrates. An immunoperoxidase stain for viral antigen was used with a hematoxylin counterstain. (Inset) The same image at a 3× higher magnification. (E) Foci of viral antigen in the spinal cord at day 14 p.i. Infected cells exhibit a morphology typical of oligodendrocytes. An immunoperoxidase stain for viral antigen was used with a hematoxylin counterstain. (F) Demyelination in the spinal cord at day 14 p.i. LFB stain was used. (G and H) Foci of viral antigen in white-matter tracks of the spinal cord at days 21 (G) and 30 (H) p.i.

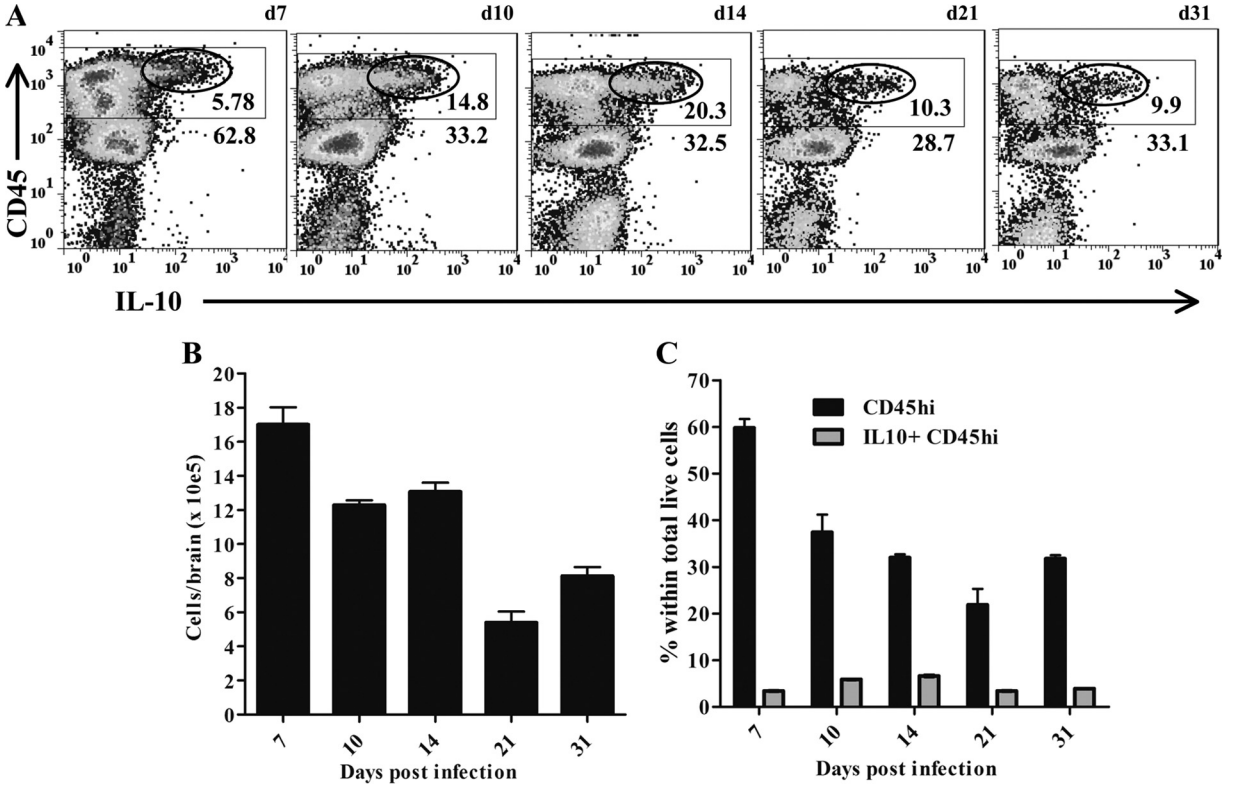

FIG. 3. Kinetics of IL-10-producing cells within the inflamed CNS. (A) Representative density plots of CNS-derived cells from infected IL-10 reporter mice. Rectangles delineate $CD45^{hi}$ inflammatory cells; numbers below rectangles give the percentages of the $CD45^{hi}$ populations within total live cells. Ellipses delineate IL-10-producing cells; numbers below ellipses give the relative percentages of IL-10-producing cells within $CD45^{hi}$ cells. Cells from 3 to 5 individual mice were pooled at each time point; d, day. Data are representative of 4 separate experiments with similar results. (B) Relative numbers of viable cells recovered from brains. (C) Percentages of $CD45^{hi}$ (filled bars) and $CD5^{hi}$ IL-10^+ (shaded bars) cells within the total live-cell population. Data from pooled samples of 4 to 5 individuals at each time point represent averages ± SEM from 4 separate experiments.

Virus-specific $CD8^+$ T cells are the major source of IL-10 during influenza virus infection of the lung (39). These data contrast with minimal IL-10 production by $CD8^+$ T cells following systemic LCMV infection (10, 14). We thus further determined the contribution of virus-specific $CD8^+$ T cells reactive to the H-$2D^d$ viral spike protein-derived epitope S510 (4, 11) to IL-10 production. Virus-specific D^b/S510 tetramer-positive $CD8^+$ T cells constituted 45 to 70% of $CD8^+$ T cell infiltrates, and this proportion remained stable during viral persistence (Fig. 6). Furthermore, the vast majority of IL-10^+ $CD8^+$ T cells were tetramer positive throughout infection. While ~25% of tetramer-positive cells produced IL-10 during the acute phase, this population declined to ~12% by day 21 p.i. By contrast, IL-10 production by the tetramer-negative $CD8^+$ T cell population with unknown specificity remained relatively constant at ~10% throughout infection. The vast majority of $CD8^+$ T-cell-derived IL-10 was thus attributed to the cells responding to the H-2^b-restricted spike protein epitope (4, 11).

Dynamic alteration in IL-10-producing $CD4^+$ T cells during JHMV infection. $CD4^+$ T cells recruited into the CNS in response to JHMV-induced encephalomyelitis are composed of both $CD25^-$ and $CD25^+$ cells. Of $CD25^+$ $CD4^+$ T cells, ~40% produced IL-10 at day 10 p.i. (Fig. 7B). At day 10 p.i., the peak of $CD4^+$ T cell infiltration, the vast majority of $CD25^+$ $CD4^+$ T cells also expressed Foxp3 (Fig. 7A). This frequency of ~80% was sustained during viral persistence (Fig. 7A). To investigate whether this is the predominant IL-10-producing population during viral encephalomyelitis, IL-10 expression was assessed in the respective $CD25^+$ and $CD25^-$ $CD4^+$ T cell subsets (Fig. 7B and D). The relative proportion of $CD25^+$ T cells within the $CD4^+$ T cell population was maximal at day 7 p.i. and remained elevated at ~15% at days 10 to 31 p.i. (Fig. 7C). As the proportion of $CD25^+$ $CD4^+$ T cells declined during the transition into persistence, the stable frequency of ~30% IL-10-producing cells within this population was maintained, resulting in an overall decline in the level of $CD25^+$ IL-10^+ cells within the $CD4^+$ T cell population (Fig. 7D). By contrast, the frequency of $CD25^-$ IL-10^+ cells within the $CD4^+$ T cell population increased from <10% at day 7 p.i. to ~30% at day 10 p.i. and remained elevated at this level thereafter. Thus, focusing only on the IL-10^+ $CD4^+$ population, the fraction of $CD25^+$ cells prevailed at a ratio of 1.9 ($CD25^+$ to $CD25^-$) at day 7 p.i., declined to 0.5 at day 10, and remained at ~0.4 throughout persistence. These data demonstrate a dynamic alteration within IL-10-producing $CD4^+$ T cells, by which the rapidly recruited, predominant $CD25^+$ $CD4^+$ T cells are supplanted by $CD25^-$ $CD4^+$ T cells.

IL-10-producing cells are preferentially retained at the site of viral persistence. JHMV persists in both the brain and the

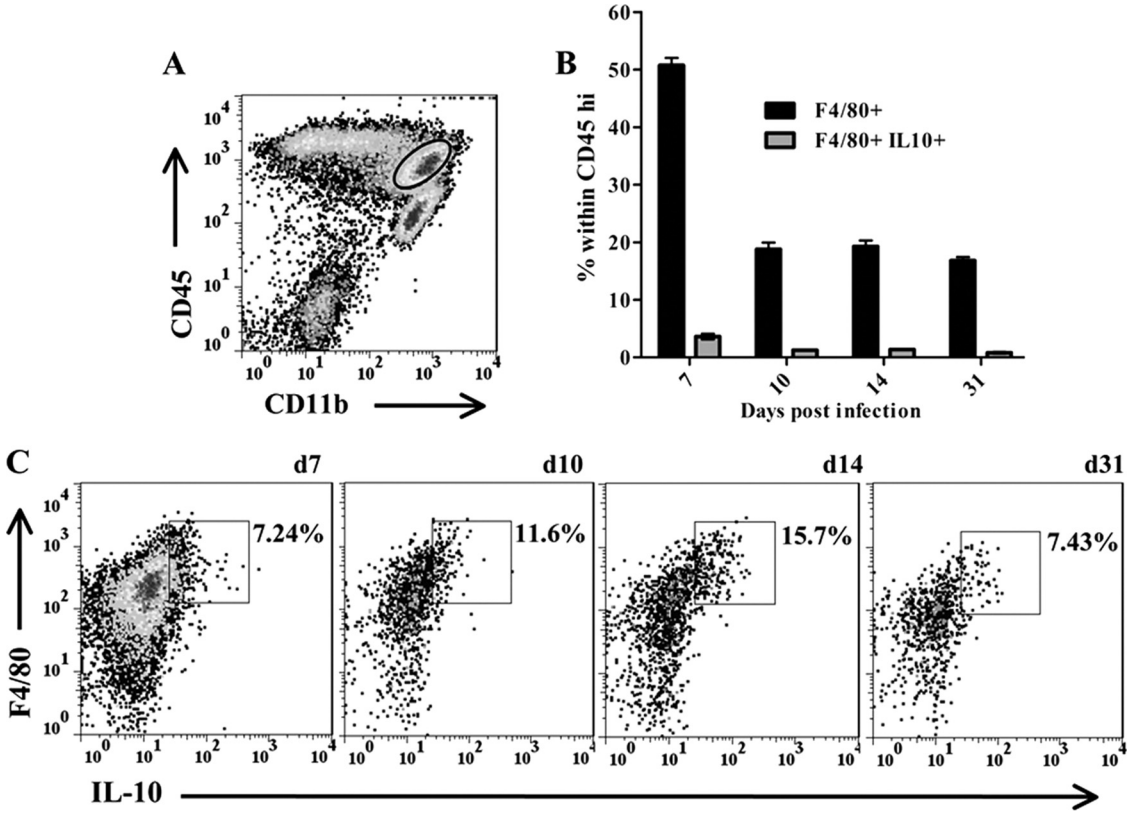

FIG. 4. Kinetics of IL-10 production in myeloid infiltrating cells. (A) Representative density plot of $CD45^{hi}$ $CD11b^{+}$ myeloid cells (circled) within total brain-derived cells at day 7 p.i. (B) Percentages of $CD11b^{+}$ $F4/80^{+}$ (filled bars) and $IL\text{-}10^{+}$ $CD11b^{+}$ $F4/80^{+}$ (shaded bars) macrophages within the $CD45^{hi}$ population at various times p.i. Data are means ± SEM from 2 separate experiments. (C) Representative density plots gated on $CD45^{hi}$ $CD11b^{+}$ cells showing F4/80 and IL-10 expression at the indicated times p.i. d, day. Rectangles delineate $IL\text{-}10^{+}$ $F4/80^{+}$ populations, and numbers give their relative percentages. Data at each time point are from 3 to 5 individual mice. Results are representative of 3 separate experiments.

spinal cord; however, the spinal cord is the primary site of viral persistence (5, 25, 34). Therefore, the relative retention of IL-10 mRNA and protein production in the spinal cord was determined during viral persistence. The kinetics of IL-10 mRNA expression in the spinal cord closely resembled that in the brain, with the level of persisting IL-10 mRNA elevated 45-fold over that for naïve mice (Fig. 8A). Although total cell yields were lower than those from the brain, the frequency of inflammatory cells was higher in the spinal cord than in the brain (Fig. 8B). In addition, the relative percentages of total T cells were higher within the spinal cord infiltrates, consistent with an ongoing inflammatory environment at the site of viral persistence (Fig. 8B). Moreover, in contrast to the results for the brain, the percentages of $CD8^{+}$ T cells were equal to, or prevailed over, those of $CD4^{+}$ T cells within $CD45^{hi}$ infiltrates in the spinal cord. Despite the higher frequencies of D^{b}/S510 tetramer-positive cells within the $CD8^{+}$ T cell population in the spinal cord than in the brain at day 21 p.i. (75% versus 58%), the proportions of $IL\text{-}10^{+}$ $CD8^{+}$ cells were diminished, comprising only 5% of T cells and <3% of the infiltrates (Fig. 8B and C). By contrast, although the frequencies of $CD4^{+}$ T cells in brain and spinal cord infiltrates were similar at days 21 and 35 p.i. (Fig. 8B), the relative percentage of $IL\text{-}10^{+}$ cells within $CD4^{+}$ T cells was higher in the spinal cord (Fig. 8D). In addition, the majority of $CD25^{+}$ $CD4^{+}$ T cells (~70%) secreted IL-10, while the frequency of IL-10-producing $CD25^{-}$ $CD4^{+}$ T cells was ~40%. These data demonstrate an even greater dominance of IL-10-producing $CD4^{+}$ relative to $CD8^{+}$ T cells in the persistently infected spinal cord compared to the brain (Fig. 8D). The increased ratio of $CD25^{+}$ to $CD25^{-}$ cells within total $IL\text{-}10^{+}$ $CD4^{+}$ T cells in the spinal cord (0.6 versus 0.2 in the brain) further suggests the possibility that both $CD25^{+}$ and $CD25^{-}$ $CD4^{+}$ T cells are major contributors of IL-10 at the site of viral persistence.

DISCUSSION

IL-10, a major anti-inflammatory cytokine, plays a critical role during infections with viruses, parasites, bacteria, and fungi (8, 13, 17, 23, 29, 37). During acute infection, IL-10 regulates immune activation, exerting an anti-inflammatory activity that minimizes tissue destruction but may also reduce the effectiveness of antiviral immunity (8, 10, 13, 15, 17, 43). Infection with glial-tropic JHMV results in the rapid activation of innate immunity (21) and initial recruitment of NK cells, neutrophils, and macrophages (5). Although NK cells are activated by IL-10 (29), previous results have demonstrated that NK cells play no role in JHMV pathogenesis, and few are retained during viral persistence (46). These initial events are followed by activation of adaptive immune effectors in the CLN (28),

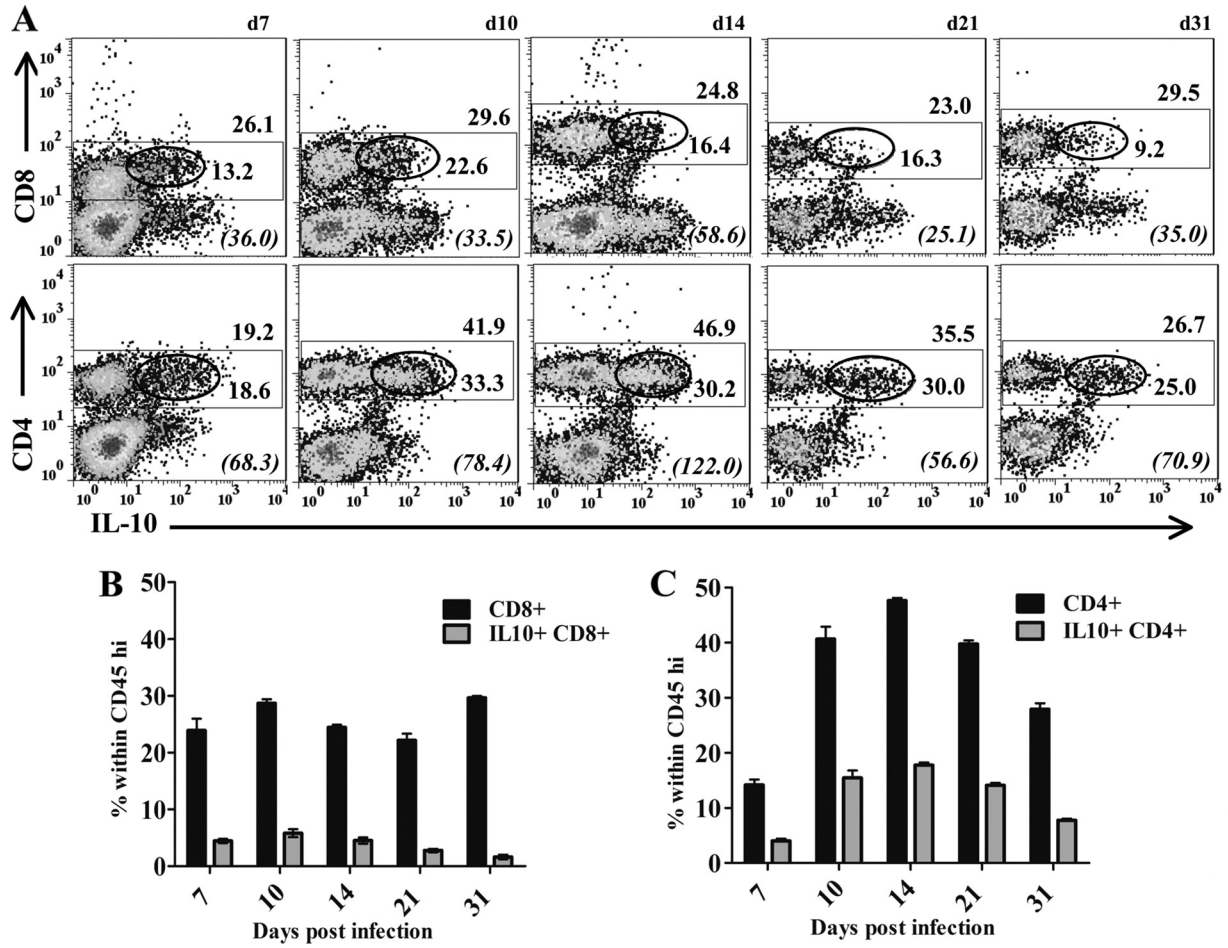

FIG. 5. CD4$^+$ T cells are the major source of IL-10 during JHMV infection. (A) Representative density plots of IL-10-producing CD8$^+$ T cells (top) and CD4$^+$ T cells (bottom) in the CNS. Plots are gated on CD45^{hi} inflammatory cells as shown in Fig. 3A. Rectangles delineate CD8$^+$ or CD4$^+$ T cell populations; ellipses delineate IL-10-producing cells within the respective T cell subset. Numbers above rectangles give the percentage of the CD8$^+$ or CD4$^+$ population within infiltrating cells; numbers below ellipses give the relative percentage of IL-10-producing cells within the T cell subset. Italicized numbers in parentheses represent the GFP MFI of IL-10$^+$ populations. Samples were pooled from 4 to 6 individuals at each time point. Results are representative of 4 separate experiments. (B and C) Relative percentages of CD8$^+$ (B) or CD4$^+$ (C) T cells (filled bars) and IL-10$^+$ CD8$^+$ or IL-10$^+$ CD4$^+$ T cells (shaded bars), respectively, within the CNS-infiltrating population at various times p.i. Data are mean percentages ± SEM from 3 to 5 experiments.

resulting in an acute encephalomyelitis associated with immune-mediated destruction of myelin (5, 25, 35, 45). Although the immune response controls infectious JHMV, sterile immunity is not achieved, resulting in a persistent CNS infection associated with ongoing demyelination, primarily in spinal cords (5, 25).

The role of IL-10 in diminishing inflammation during acute CNS infection in an attempt to limit potential damage, and

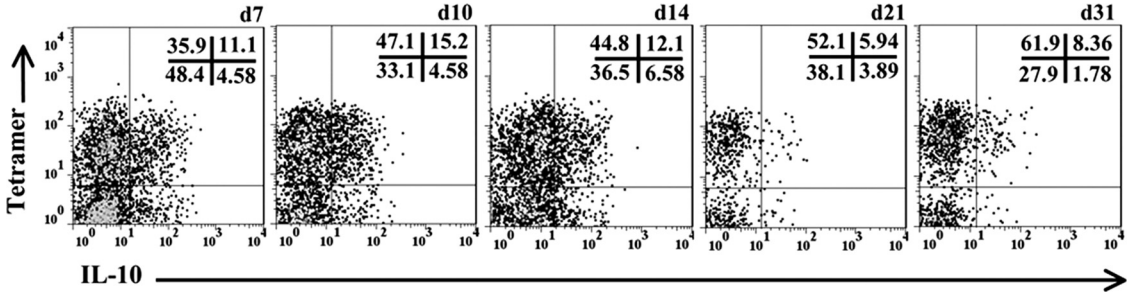

FIG. 6. IL-10 production by virus-specific CD8$^+$ T cells during JHMV infection. Representative density plots, gated on CD45^{hi} CD8$^+$ T cells, show IL-10 production within virus-specific cells. Numbers represent percentages in the respective quadrants. Samples were pooled from 4 to 6 individuals at each time point. d, day. Results are representative of 4 separate experiments with similar results.

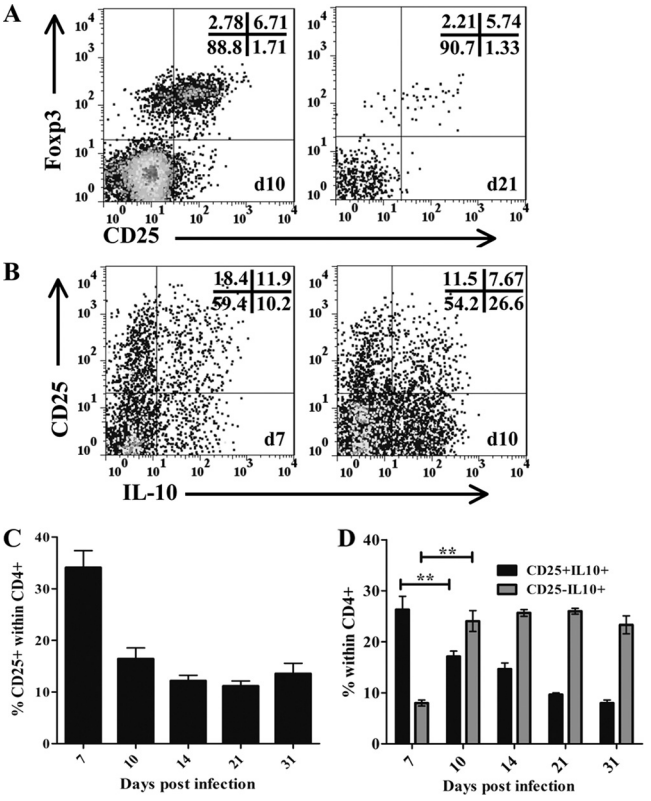

FIG. 7. Shift in IL-10-producing CD4 T cell populations during viral pathogenesis. (A) Representative density plots, gated on $CD45^{hi}$ $CD4^+$ T cells, depicting CD25 expression and intracellular Foxp3 expression at days (d) 10 and 21 p.i. (B) Representative density plots, gated on $CD45^{hi}$ $CD4^+$ T cells, depicting IL-10-producing $CD25^+$ and $CD25^-$ cells at days 10 and 21 p.i. (C) Relative percentages of $CD25^+$ cells within $CD4^+$ T cells. (D) Relative percentages of $CD25^+$ $IL\text{-}10^+$ (filled bars) and $CD25^-$ $IL\text{-}10^+$ (shaded bars) cells within $CD4^+$ T cells at various times p.i. Samples were pooled from 4 to 6 mice at each time point. Results are means ± SEM from 4 separate experiments. **, $P < 0.005$.

thus inadvertently sparing the host from mortality but facilitating the transition from acute to persistent infection, is unclear. Recent data suggest that increased $CD8^+$ T cell activity in the absence of inhibitory molecules is associated with enhanced viral control, albeit at the cost of increased tissue damage and mortality (34). Furthermore, recently published results also indicate that IL-10 is prominently secreted by $CD8^+$ T cells with high lytic activity. In the absence of IL-10, CNS inflammation and mortality are increased following JHMV infection (26, 41), consistent with an anti-inflammatory role of IL-10. The role of IL-10 in regulating infectious JHMV within the CNS is currently unclear. It was initially reported to differ both from the role in systemic viral infections (10, 14, 32, 33) and from the role in viral infection of the lung (39) in that the viral load increased during acute JHMV infection in the absence of IL-10 (26). These data suggested that IL-10 regulation and its effects during viral encephalitis differ from those for infections at other sites. However, recent data indicate that the virus is cleared more rapidly, possibly due to increased activity of IL-10-secreting virus-specific $CD8^+$ T cells (1). The present experiments were undertaken using an IL-10 reporter mouse in which IL-10 production is preserved in order to define the cell types producing IL-10 and the kinetics of their appearance in the inflamed CNS during acute sublethal virus-induced encephalomyelitis. The fact that the pathological hallmarks, viral control, and recruitment of CNS immune cells were similar to those for wt mice (5) validate unaltered disease in these mice.

Macrophages, microglia, dendritic cells, B cells, and both $CD4^+$ and $CD8^+$ T cells are capable of IL-10 production (2, 13, 14, 22, 29). A minimal number of monocytes recruited into the CNS expressed IL-10 during acute JHMV encephalomyelitis; however, they remained at low levels during persistence. Surprisingly, microglia, which constitute a potential CNS-resident antigen-presenting cell population, were also only sparse IL-10 producers, even though increased major histocompatibility complex class II expression indicated cellular activation (data not shown). It is also intriguing that JHMV infection induced a rapid increase in the level of IL-10 mRNA within the CNS, which peaked prior to the detection of IL-10-secreting inflammatory cells. Although IL-10 mRNA expression may not be an accurate reflection of protein synthesis (29), these data may also reflect the attempt of the CNS-resident cells to limit immune-mediated damage. Nevertheless, the absence of a significant increase in IL-10 production by myeloid cells following JHMV infection differs from systemic infection by LCMV, in which increased IL-10 production by dendritic cells is associated with viral persistence (10, 14, 15, 17).

Our data demonstrate that, in contrast to the monocyte/macrophage and microglial myeloid populations, T cells are the primary source of IL-10 in the CNS during acute JHMV infection. A low frequency of $CD8^+$ T cells produced IL-10, with the majority specific for the S510 viral epitope, at all time points p.i. The decline in IL-10 production as the virus was controlled is consistent with IL-10 production by $CD8^+$ T cells during influenza virus infection of the lung (39). However, in contrast to influenza virus infection, in which $CD8^+$ T cells constituted the largest IL-10-producing population (39), $CD4^+$ T cells harbored the highest frequency of IL-10-producing cells during viral acute encephalomyelitis. Within the $CD4^+$ T cell population, both $CD25^+$ and $CD25^-$ T cells produced IL-10, suggesting diverse regulatory capacities and potentially divergent roles in preventing tissue destruction. $CD25^+$ $CD4^+$ T cells, the major population producing IL-10 during acute infection, comprise both effector $CD4^+$ T cells and $Foxp3^+$ natural regulatory T cells (Treg). Treg, which play a critical role in homeostasis but express a limited TcR repertoire, are one source of IL-10 (16, 22). During acute infection, Treg both diminish the severity of JHMV-induced disease (1) and inhibit the inflammatory response, resulting in a concomitant decrease in immune-mediated demyelination (45). The data presented here demonstrate that the vast majority of $CD25^+$ $CD4^+$ T cells recruited into the CNS express Foxp3. These results not only support the concept that IL-10 secretion by Treg may limit tissue destruction within the CNS but also suggest a minimal contribution of $CD25^+$ $CD4^+$ effector T cells to overall IL-10 levels during acute infection.

Anti-inflammatory responses are widely thought to contribute to viral persistence in both humans and mice (8, 13, 15, 17). IL-10 and the inhibitory programmed death ligand 1 (PD-L1) have been implicated in the facilitation of diverse persistent viral infections, including those established by human immu-

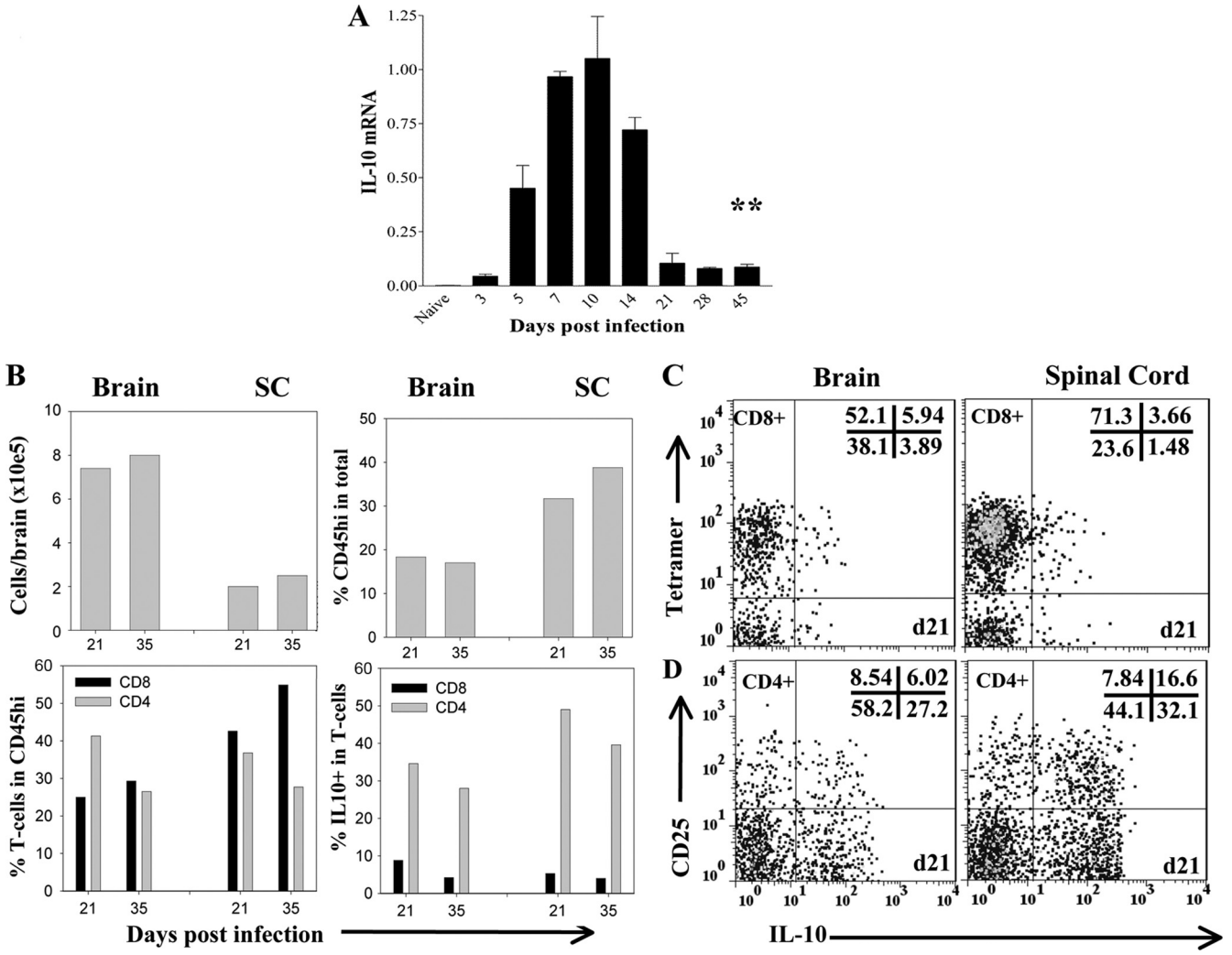

FIG. 8. IL-10-producing $CD4^+$ T cells preferentially accumulate in the spinal cord during JHMV persistence. (A) IL-10 mRNA expression in spinal cords at various times p.i. assessed by qRT-PCR. Asterisks indicate a significant difference (**, $P < 0.005$) from results for naïve mice. Data are expressed relative to the level of GAPDH mRNA. Expression in naïve mice is 0.0018 ± 0.00026. (B) Plots depicting the total numbers of viable cells recovered from the brain and spinal cord (SC) (top left), the percentages of $CD45^{hi}$ inflammatory cells within live cells (top right), the relative percentages of $CD4^+$ and $CD8^+$ T cells within $CD45^{hi}$ cells (bottom left), and the relative percentages of IL-10^+ cells within each T cell subset during viral persistence (bottom right). Samples were pooled from 4 to 6 individual mice at each time point. Results are representative of 4 separate experiments. (C and D) Comparison of IL-10 production by tetramer-positive $CD8^+$ T cells (C), $CD25^+$ $CD4^+$ T cells, and $CD25^-$ $CD4^+$ T cells (D) in the brain (left) and spinal cord (right) at day (d) 21 p.i. Data are representative of 3 separate experiments with similar results.

nodeficiency virus, hepatitis C virus, cytomegalovirus, and LCMV (7, 10, 17, 23). PD-L1 regulates JHMV infection by limiting virus clearance and ameliorating tissue destruction (34), a role similar to that of IL-10 in reducing influenza virus-mediated pathology of the lung (39). During the transition from acute to persistent systemic LCMV infection, the frequency of IL-10-producing T cells declines, concomitantly with an increase in the frequency of IL-10-producing dendritic cells (10, 14, 17). In stark contrast, the transition from acute to chronic JHMV infection was not associated with an alteration in IL-10 production by potential antigen-presenting cells. This difference may reflect T cell exhaustion during LCMV infection (8, 15), which is not evident during JHMV persistence characterized by a low antigen load (5). Nevertheless, as in the transition from acute to persistent LCMV infection (7, 10, 14), the frequency of $CD8^+$ T cells producing IL-10 declines within the CNS as persistent JHMV infection is established. Whether this coincides with prolonged PD-L1 expression on oligodendroglia, the major cell type harboring persistent virus (5, 34, 44), remains to be elucidated.

JHMV initially replicates in the parenchyma and ependymal cells of the brain (44). However, as inflammation increases, virus infection progresses into the spinal cord canal, subsequently attacking oligodendroglia, resulting in the hallmark demyelination associated with this infection. Adaptive immunity controls infectious virus in both the brain and the spinal cord but is unable to eliminate the virus from oligodendroglia (44). Although the virus persists at low levels in the brain itself, persistence is more prolonged and is associated with ongoing pathology, predominantly in the spinal cord (28, 34). The role

of IL-10-producing $CD4^+$ T cells in the regulation of JHMV persistence was supported by analysis of the spinal cord. $CD4^+$ and $CD8^+$ T cells producing IL-10 are preferentially retained in the spinal cord versus the brain during persistence; however, the majority of cells producing IL-10 are $CD4^+$ T cells. The transition from acute to persistent JHMV infection is associated with a shift from $CD25^+$ $CD4^+$ to $CD25^-$ $CD4^+$ T cells within IL-10-producing $CD4^+$ T cells, which appears to be delayed in the spinal cord. Indeed, preliminary data indicate the presence of IL-10-producing cells associated with areas of virus-induced demyelination in the spinal cord during JHMV persistence (data not shown). The increase in $CD25^-$ $CD4^+$ T cells suggests a conversion from a predominant Th1 cell response (5, 20) to a population with regulatory capacity (12, 22). These data suggest that the response to viral infection within the CNS may be similar to the IL-27-mediated induction of $CD25^-$ $CD4^+$ regulatory T cells that occurs during experimental autoimmune encephalomyelitis (18) and the induction of a $CD25^-$ $CD4^+$ regulatory population during persistent parasite infection (12, 13, 22, 30).

In summary, IL-10 production by $CD8^+$ T cells peaked during acute CNS inflammation but subsequently declined as the infection transitioned to persistence and the $CD8^+$ T cell population contracted. Nevertheless, the maintenance of IL-10 production by $CD4^+$ T cells in the CNS implied ongoing cues to sustain an anti-inflammatory environment. The mechanisms underlying the distinct temporal induction of IL-10 production by T cell subsets remain to be resolved but may provide insight into the regulation of both systemic and focal persistent viral infections. These results indicate that, in addition to the protection mediated by PD-L1 (34), the host uses multiple mechanisms, targeting distinct cell types, to reduce tissue damage at the cost of tolerating viral persistence.

ACKNOWLEDGMENTS

We thank Wenqiang Wei and Ernesto Baron for assistance with histopathology and Jennifer Powers for FACS purification.

This work was supported by U.S. National Institutes of Health grant NS 64932.

REFERENCES

1. **Anghelina, D., J. Zhao, K. Trandem, and S. Perlman.** 2009. Role of regulatory T cells in coronavirus-induced acute encephalitis. Virology **385:**358–367.
2. **Batten, M., et al.** 2008. IL-27 is a potent inducer of IL-10 but not Foxp3 in murine T cells. J. Immunol. **180:**2752–2756.
3. **Bergmann, C. C., J. D. Altman, D. Hinton, and S. A. Stohlman.** 1999. Inverted immunodominance and impaired cytolytic function of cytolytic $CD8^+$ T cells during viral persistence in the central nervous system. J. Immunol. **163:**3379–3387.
4. **Bergmann, C. C., Q. Yao, M. Lin, and S. Stohlman.** 1996. The JHM strain of mouse hepatitis virus induces a spike protein-specific Db-restricted cytotoxic T-cell response. J. Gen. Virol. **77:**315–325.
5. **Bergmann, C. C., T. E. Lane, and S. A. Stohlman.** 2006. Coronavirus infection of the central nervous system: host-virus stand-off. Nat. Rev. Microbiol. **4:**121–132.
6. **Bergmann, C. C., et al.** 2004. Perforin and gamma-mediated control of coronavirus central nervous system infection by CD8 T cells in the absence of CD4 T cells. J. Virol. **78:**1739–1750.
7. **Blackburn, S. D., et al.** 2009. Coregulation of $CD8^+$ T cell exhaustion by multiple inhibitory receptors during chronic viral infection. Nat. Immunol. **10:**29–37.
8. **Blackburn, S. D., and E. J. Wherry.** 2007. IL-10, T-cell exhaustion and virus persistence. Trends Microbiol. **15:**143–146.
9. **Brooks, D. G., et al.** 2008. IL-10 and PD-L1 operate through distinct pathways to suppress T-cell activity during persistence. Proc. Natl. Acad. Sci. U. S. A. **105:**20428–20433.
10. **Brooks, D. G., et al.** 2006. Interleukin-10 determines viral clearance or persistence in vivo. Nat. Med. **12:**1301–1309.
11. **Castro, R. F., and S. Perlman.** 1995. $CD8^+$ T-cell epitopes within the surface glycoprotein of a neurotropic coronavirus and correlation with pathogenicity. J. Virol. **69:**8127–8131.
12. **Chen, J., and X. S. Liu.** 2009. Development and function of IL-10, interferon gamma secreting $CD4^+$ T cells. J. Leukoc. Biol. **86:**1305–1310.
13. **Couper, K. N., D. G. Blount, and E. M. Riley.** 2008. IL-10: the master regulator of immunity to infection. J. Immunol. **180:**5771–5777.
14. **Ejrnaes, M., et al.** 2006. Resolution of a chronic viral infection after interleukin-10 receptor blockade. J. Exp. Med. **203:**2461–2472.
15. **Fahey, L. M., and D. G. Brooks.** 2010. Opposing positive and negative regulation of T cell activity during viral persistence. Curr. Opin. Immunol. **22:**348–354.
16. **Feuerer, M., J. A. Hill, D. Mathis, and C. Benoist.** 2009. $Foxp3^+$ regulatory T cells: differentiation, specification, subphenotypes. Nat. Immunol. **10:**689–695.
17. **Filippi, C. M., and M. G. von Herrath.** 2008. IL-10 and the resolution of infections. J. Pathol. **214:**224–230.
18. **Fitzgerald, D. C., et al.** 2007. Suppression of autoimmune inflammation of the central nervous system by interleukin-10 secreted by interleukin-27-stimulated cells. Nat. Immunol. **8:**1372–1379.
19. **Fleming, J. O., M. D. Trousdale, F. A. el-Zaatari, S. A. Stohlman, and L. P. Weiner.** 1986. Pathogenicity of antigenic variants of murine coronavirus JHM selected with monoclonal antibodies. J. Virol. **58:**869–875.
20. **Haring, J. S., L. L. Pewe, and S. Perlman.** 2001. High-magnitude, virus-specific CD4 T-cell response in the central nervous system of coronavirus infected mice. J. Virol. **75:**3043–3047.
21. **Ireland, D. D., S. A. Stohlman, D. R. Hinton, R. Atkinson, and C. C. Bergmann.** 2008. Type I interferons are essential in controlling neurotropic coronavirus infection irrespective of functional CD8 T cells. J. Virol. **82:**300–310.
22. **Jankovic, D., and G. Trinchieri.** 2007. IL-10 or not IL-10: that is the question. Nat. Immunol. **8:**1281–1283.
23. **Jones, M., et al.** 2010. IL-10 restricts memory T cell inflation during cytomegalovirus infection. J. Immunol. **185:**3583–3592.
24. **Kapil, P., et al.** 2009. Interleukin-12 (IL-12), but not IL-23 deficiency ameliorates viral encephalitis without affecting viral control. J. Virol. **83:**5978–5986.
25. **Lane, T. E., and M. P. Hosking.** 2010. The pathogenesis of murine coronavirus infection in the central nervous system. Crit. Rev. Immunol. **30:**119–130.
26. **Lin, M. T., D. R. Hinton, B. Parra, S. A. Stohlman, and R. C. van der Veen.** 1998. The role of IL-10 in mouse hepatitis virus-induced demyelinating disease. Virology **245:**270–280.
27. **Madan, R., et al.** 2009. Nonredundant roles for B cell-derived IL-10 in immune counter-regulation. J. Immunol. **183:**2312–2320.
28. **Marten, N., S. Stohlman, J. Zhou, and C. Bergmann.** 2003. Kinetics of virus specific $CD8^+$ T-cell expansion and trafficking following central nervous system infection. J. Virol. **77:**2775–2778.
29. **Moore, K. W., R. de Waal Malefyt, R. L. Coffman, and A. O'Garra.** 2001. Interleukin-10 and interleukin-10 receptor. Annu. Rev. Immunol. **19:**683–765.
30. **O'Garra, A., and P. Vieira.** 2007. T_H1 cells control themselves by producing interleukin-10. Nat. Rev. Immunol. **7:**425–428.
31. **Parra, B., D. R. Hinton, M. T. Lin, D. J. Cua, and S. A. Stohlman.** 1997. Kinetics of cytokine mRNA expression in the central nervous system following lethal and non-lethal coronavirus-induced acute encephalomyelitis. Virology **233:**260–270.
32. **Peacock, J. W., and K. L. Bost.** 2001. Murine gammaherpesvirus-68-induced interleukin-10 increases viral burden, but limits virus-induced splenomegaly and leukocytosis. Immunology **104:**109–117.
33. **Perona-Wright, G., et al.** 2009. Systemic but not local infections elicit immunosuppressive IL-10 production by natural killer cells. Cell Host Microbe **6:**503–512.
34. **Phares, T. W., S. A. Stohlman, D. R. Hinton, R. Atkinson, and C. C. Bergmann.** 2010. Enhanced antiviral T cell function in the absence of B7–H1 is insufficient to prevent persistence but exacerbates axonal bystander damage during viral encephalomyelitis. J. Immunol. **185:**5607–5618.
35. **Savarin, C., C. C. Bergmann, D. R. Hinton, R. M. Ransohoff, and S. A. Stohlman.** 2008. Memory $CD4^+$ T cell-mediated protection from lethal coronavirus encephalomyelitis. J. Virol. **82:**12432–12440.
36. **Sedgwick, J. D., A. L. Ford, E. Foulcher, and R. Airriess.** 1998. Central nervous system microglial activation and proliferation follows direct interaction with tissue infiltrating T cell blasts. J. Immunol. **160:**5320–5330.
37. **Sher, A., D. Fiorentino, P. Caspar, E. Pearce, and T. Mosmann.** 1991. Production of IL-10 by $CD4^+$ T lymphocytes correlates with down-regulation of Th1 cytokine synthesis in helminth infection. J. Immunol. **147:**2713–2716.
38. **Slifka, M. R., F. Rodriguez, and J. L. Whitton.** 1999. Rapid on/off cycling of cytokine production by virus-specific $CD8^+$ T cells. Nature **401:**76–79.
39. **Sun, J., R. Madan, C. L. Karp, and T. J. Braciale.** 2009. Effector T cells

control lung inflammation during acute influenza virus infection by producing IL-10. Nat. Med. **15:**277–284.

40. **Trandem, K., D. Anghelina, J. Zhao, and S. Perlman.** 2010. Regulatory T cells inhibit T cell proliferation and decrease demyelination in mice chronically infected with a coronavirus. J. Immunol. **184:**4391–4400.
41. **Trandem, K., J. Zhao, E. Fleming, and S. Perlman.** 2011. Highly activated cytotoxic CD8 T cells express IL-10 at the peak of coronavirus-induced encephalitis. J. Immunol. **186:**3642–3652.
42. **Tschen, S., et al.** 2006. CNS viral infection diverts homing of antibody-secreting cells from lymphoid organs to the CNS. Eur. J. Immunol. **36:**603–612.
43. **van Den Broek, M., et al.** 2000. IL-4 and IL-10 antagonize IL-12-mediated protection against acute vaccinia virus infection with a limited role of IFN-γ and nitric oxide synthetase 2. J. Immunol. **164:**371–378.
44. **Wang, F. I., D. R. Hinton, W. Gilmore, M. D. Trousdale, and J. O. Fleming.** 1992. Sequential infection of glial cells by the murine hepatitis virus JHM strain (MHV-4) leads to a characteristic distribution of demyelination. Lab. Invest. **66:**744–754.
45. **Wu, G. F., A. A. Dandekar, L. L. Pewe, and S. Perlman.** 2000. CD4 and CD8 T cells have redundant but not identical roles in virus induced demyelination. J. Immunol. **165:**2278–2286.
46. **Zuo, J., et al.** 2006. Mouse hepatitis virus pathogenesis in the central nervous system is independent of IL-15 and natural killer cells. Virology **350:**206–215.